Speciation Equilibria, Clustering, and Chemical-Exchange Kinetics in Non-Oxide Glasses and Melts. High-Temperature ^{31}P NMR Study of the System Phosphorus–Selenium

Robert Maxwell and Hellmut Eckert*

Contribution from the Department of Chemistry, University of California, Santa Barbara, California 93106

Received October 8, 1992

Abstract: Speciation equilibria and dynamic exchange processes occurring in phosphorus–selenium melts above the glass transition temperature are characterized by in-situ static ^{31}P NMR over the temperature range 25 °C $\leq T \leq$ 650 °C. In glasses with low phosphorus contents, the spectra monitor the decomposition of tetrahedral $Se{=}PSe_{3/2}$ units occurring at temperatures below 200 °C. In glasses with phosphorus contents $\geq$ 40 atom %, within the temperature region 200 °C $\leq T \leq$ 350 °C, a network depolymerization process occurs, leading to the creation of molecular P_4Se_3 units. This process can be described by a phenomenological equilibrium constant, whose experimental temperature dependence indicates a reaction enthalpy of 30–40 kJ/mol. Above 400 °C the experimental spectra are affected by chemical exchange between molecular P_4Se_3 and the molten-glass matrix. The temperature-dependent rate constants derived from explicit line-shape simulations yield an activation energy of 116 kJ/mol for this process. Extrapolation of these temperature-dependent processes to the glass transition temperature indicates that P–Se glasses with phosphorus concentrations below 50 atom % generally show little evidence for intermediate-range order, except for some polymerized P_4Se_3-precursor states within the concentration range 40–50 atom % P. The kinetic data further suggest the glass transition in the P–Se system is associated with slow chemical exchange processes associated with bond breakage/bond formation, as previously shown for silicate glasses.

Introduction

The development of infrared-transparent materials operating in the wavelength range beyond the 1.8-μm limit of silica-based glass fibers is an important goal of current optical fiber research, and non-oxide chalcogenide glasses based on the sulfides, selenides, tellurides, and pnictides of the main group III–V elements recently have gained much interest due to their wide transparency window in the 2–10 μm wavelength region.[1] Such glasses offer a host of technologically interesting properties including reversible conductivity switching induced by electric fields,[2] defect controlled semiconducting properties,[3] and fast ionic conduction suitable for solid electrolyte applications.[4] By varying the composition and thermal history of these materials, their properties can be tailored to cover a wide range of different technological applications.

Most of the research conducted on non-oxide chalcogenide systems prior to 1980 concentrated on establishing phase diagrams, determining regions of glass formation, and characterizing thermodynamic and physicochemical properties.[5] Driven by the search for structural guidelines to optimize materials properties, it is only recently that the structure of these glasses has moved into the focus of scientific attention.[6] On the basis of extensive spectroscopic[7] and theoretical[8] structural studies during the past decade, general structural concepts for these glasses now are emerging slowly. There is general agreement that neither the continuous random network model[9] (applicable to silicate glasses) nor the random-sphere close-packing model[10] (applicable to certain metallic glasses) can provide a realistic description of the structure of non-oxide chalcogenide glasses.[11] New conceptual approaches have addressed the question of short-range order on the basis of average valences and coordination numbers,[12] while the theoretical framework of rigidity percolation[13] has been applied to explain macroscopic properties of covalent networks.[14] Experimentally, EXAFS and diffraction studies appear to indicate the presence of substantial intermediate-range order on the 10–20-Å scale in many covalent glasses,[15] whereas solid-state-NMR results signify chemical disorder, i.e. the competition of homopolar and heteropolar bonding as an essential feature of glass formation in these systems.[16]

Glasses in the phosphorus–selenium system have been the subject of considerable interest and controversy for approximately two decades.[17] Most recently, evidence from neutron diffraction and Raman spectroscopy has shown that vitreous P_2Se is an

(1) Taylor, P. C. *Mater. Res. Soc. Bull.* **1987**, 36. Nishii, J.; Morimoto, S.; Inagawa, I.; Iizuka, R.; Yamishita, T.; Yamagashi, T. *J. Non-Cryst. Solids* **1992**, *140*, 199.
(2) Ovshinsky, S. R. *Phys. Rev. Lett.* **1968**, *21*, 1450.
(3) Kastner, M. *J. Non-Cryst. Solids* **1980**, *35–36*, 807. Adler, D. *J. Non-Cryst. Solids* **1985**, *73*, 205 and references therein.
(4) Pradel, A.; Ribes, M. *Solid State Ionics* **1986**, *18/19*, 351. Zhang, Zh.; Kennedy, J. *Solid State Ionics* **1990**, *38*, 217.
(5) Hilton, A. R.; Jones, C. E.; Brau, M. *Phys. Chem. Glasses* **1966**, *7*, 105. Kolomiets, B. T. *Phys. Status Solidi* **1964**, *7*, 359, 713. Borisova, Z. U. *Glassy Semiconductors*; Plenum Press: New York, 1981; and references therein.
(6) Comprehensive discussions of the structural problem in glasses can be found in: Zallen, R. *The Physics of Amorphous Solids*; John Wiley & Sons: New York, 1983. Weeks, R. A. *J. Non-Cryst. Solids* **1985**, *73*, 103.
(7) Elliott, S. R. *Nature (London)* **1992**, *354*, 445. Armand, P.; Ibanez, A.; Dexpert, H.; Philippot, E. *J. Non-Cryst. Solids* **1992**, *139*, 137. Mastelaro, V.; Dexpert, H.; Benazzeth, S.; Ollitrault-Fichet, R. *J. Solid State Chem.* **1992**, *96*, 301.
(8) Angell, C. A. *J. Non-Cryst. Solids* **1985**, *73*, 1. Vashishta, P.; Kalia, R. K.; Ebbsjö, I. *J. Non-Cryst. Solids* **1988**, *106*, 301. Antonio, G. A.; Kalia, R. K.; Vashishta, P. *J. Non-Cryst. Solids* **1988**, *106*, 305.
(9) Zachariasen, W. W. *J. Am. Ceram. Soc.* **1932**, *54*, 3841.
(10) Cargill, G. S. *J. Appl. Phys.* **1970**, *41*, 2248. Cohen, M. H.; Turnbull, D. *Nature* **1964**, *203*, 964.
(11) Boolchand, P. *Hyperfine Interact.* **1986**, *27*, 3.
(12) Liu, Z.; Taylor, P. C. *Solid State Commun.* **1989**, *70*, 81.
(13) Thorpe, M. F. *J. Non-Cryst. Solids* **1985**, *76*, 109. Phillips, J. C. *J. Non-Cryst. Solids* **1979**, *34*, 153.
(14) Tatsumisago, M.; Halfpap, B. L.; Green, J. L.; Lindsay, S. M.; Angell, C. A. *Phys. Rev. Lett.* **1990**, *64*, 1549.
(15) Elliott, S. R. *Nature (London)* **1992**, *354*, 445. Phillips, J. C. *J. Non-Cryst. Solids* **1981**, *43*, 37.
(16) Eckert, H. *Prog. Nucl. Magn. Reson. Spectrosc.* **1992**, *24*, 159. Eckert, H. *Angew. Chem. Adv. Mater.* **1989**, *101*, 1763.
(17) Blachnik, R.; Hoppe, A. *J. Non-Cryst. Solids* **1979**, *34*, 191.

0002-7863/93/1515-4747$04.00/0

interesting example of a zero-dimensional glass, i.e. a disordered assembly mainly comprised of P_4Se_x molecular units.[18,19] However, the structure of glasses in the selenium-rich domain (≤50 atom % P) is still a point of controversy. While EXAFS and neutron diffraction data suggest that these glasses consist of well-defined P_4Se_3, P_4Se_4, and P_4Se_5 cluster units embedded in a selenium-rich matrix,[20] solid-state-NMR studies indicate that such intermediate-range-order structures are far less abundant than previously believed.[21-23] On the other hand, the idea of intermediate-range order and clustering has been reinforced by recent high-temperature NMR studies in the related phosphorus–sulfur system.[24] These results have revealed unambiguously that at certain compositions (45 and 50 atom % P) the molten states are essentially mixtures of molecular P_4S_x species. Similarly, previous high-temperature studies by Stebbins and co-workers have contributed to a much deeper understanding of the structural and thermodynamic behavior of molten silicates.[25]

It is important to realize that all of the above structural findings, carried out on melt-quenched glasses, reflect the thermodynamics of the molten states as they are frozen at the glass transition temperature, T_g. In pursuit of a more detailed understanding of the structure of P–Se glasses, it is therefore necessary to characterize the underlying melt equilibria determining the structure of these glasses by in-situ temperature-dependent studies above T_g. To resolve the contradictions in the literature and to provide some firm answers regarding the extent of clustering and intermediate-range order in phosphorus–selenium glasses, we report here the results of a systematic high-temperature NMR study of this system.

Experimental Section

Sample Preparation and Characterization. Phosphorus–selenium glasses containing 13, 30, 40, 45, and 48 atom % P were prepared within evacuated quartz ampules, heated above 650 °C for at least 48 h, and either cooled slowly in a furnace or quenched rapidly in ice–water. Glass transition temperatures (T_g) were measured on a Dupont 912 dual sample differential scanning calorimeter, using heating rates of 5–10 °C/min. All of the glasses studied exhibit single T_g's in agreement with the literature and show no sign of recrystallization under DSC conditions. Formation of completely amorphous samples was further verified by X-ray powder diffraction, using a Scintag diffractometer. All sample manipulations were carried out in a glovebox under an anhydrous Ar atmosphere.

Crystalline α-P_4Se_3 was obtained by slow cooling of a melt containing a stoichiometric ratio of P and Se and subsequent recrystallization of the product from anhydrous carbon disulfide (HPLC grade). The identity and purity of the product was verified by differential scanning calorimetry (mp 246 °C, lit. 247 °C), X-ray powder diffraction, and liquid-state NMR (doublet at −106 ppm and quartet at 37 ppm vs 85% H_3PO_4), in good agreement with literature data.

NMR Studies. Variable-temperature (VT) NMR spectra were obtained at 121.66 and 81.01 MHz, using General Electric GN-300 and modified Bruker CXP-200 spectrometers equipped with a VT static probe manufactured by Doty-Scientific. Single-pulse spectra were acquired with $\pi/4$ pulse lengths of 4 μs to ensure quantitative results over the spectral window of interest. Temperatures were allowed to equilibrate for ca. 30 min, and no appreciable temperature hysteresis effects were noted under such conditions. Recycle delays ranged from a few minutes at $T < 200$ °C to less than 100 ms at $T > 400$ °C. In samples with low phosphorus contents at low temperatures, background distortions were noted, albeit less severely at 81.01 MHz. Ice–water-quenched samples were studied at 121.66 MHz and oven-quenched samples at 81.01 MHz, within the temperature range 25 °C ≤ T ≤ 650 °C. No significant influence of the cooling rate was observed. The model compound α-P_4Se_3 was studied at both frequencies, within the temperature range 25 °C ≤ T ≤ 650 °C.

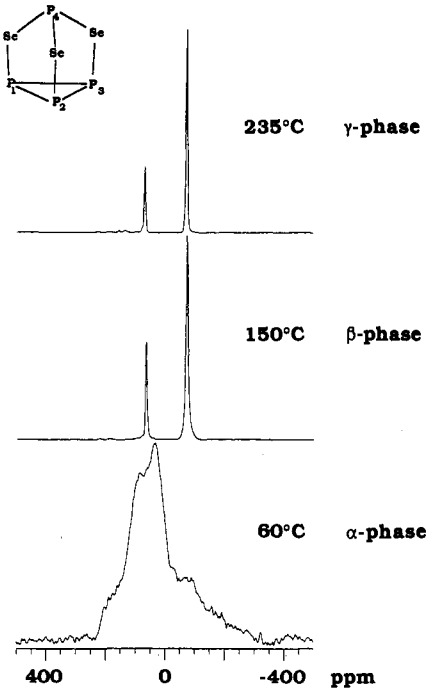

Figure 1. 121.66 MHz static solid-state ^{31}P NMR spectra of three crystalline modifications of P_4Se_3.

Results, Data Analysis, and Interpretation

Variable-Temperature ^{31}P NMR Studies of Crystalline P_4Se_3. P_4Se_3 exhibits two phase transitions before it melts at 247 °C. The low-temperature α-phase, which can only be obtained by crystallization from solvents, undergoes a first-order phase transition to the plastic crystalline β-phase at 85 °C. This compound crystallizes in the space group $R3m$ and has a structure related to that of β-Mn. At 207 °C β-P_4Se_3 undergoes a more subtle structural rearrangement to the γ-phase, which is presumed to have cubic symmetry.[26] If the material is cooled from the melt, a more disordered phase β'-P_4Se_3 is obtained, which remains stable at room temperature and transforms on heating to the γ phase at 192 °C.[27] Figure 1 shows the static NMR spectra of these phases at temperatures above the respective phase transitions. The transition from the α- to the β-phase is easily noted by the obvious change in solid-state powder patterns. The α-phase is characterized by a broad asymmetric resonance centered near 0 ppm. This spectrum comprises the dipolar chemical shift powder patterns of P atoms in the four crystallographically inequivalent molecules present in the asymmetric unit.[28] Magic-angle-spinning (MAS) NMR spectra of this compound have been previously reported.[23,29] In stark contrast, the static solid-state NMR spectra of β- and β'-P_4Se_3 are characterized by two rather narrow resonances around 62 and −76 ppm in a 1:3 ratio, assigned to the one apical, δ_4, and the three basal phosphorus atoms, $\delta_{1,2,3}$, respectively. The dramatic differences between the NMR spectra for the α- and β-phases are due to differences in molecular mobility. The homonuclear ^{31}P–^{31}P dipolar broadening and chemical shift anisotropy effects present in the spectrum of the α-phase are averaged to zero by rapid isotropic reorientation of the P_4Se_3 molecules above the phase transition. A similar situation

(18) Verrall, D. J.; Elliott, S. R. *J. Non-Cryst. Solids* **1989**, *114*, 34. Verall, D. J.; Elliott, S. R. *J. Non-Cryst. Solids* **1988**, *106*, 47.
(19) Phillips, T. R.; Wolverson, D.; Burdis, M. S.; Fang, Y. *Phys. Rev. Lett.* **1989**, *63*, 2574.
(20) Price, D. L.; Misawa, M.; Susman, S.; Morrison, T. I.; Shenoy, G. K.; Grimsditch, M. *J. Non-Cryst. Solids* **1984**, *66*, 443. Arai, M.; Johnson, R. W.; Price, D. L.; Susman, S.; Gay, M.; Enderby, J. E. *J. Non-Cryst. Solids* **1986**, *83*, 80.
(21) Lathrop, D.; Eckert, H. *J. Am. Chem. Soc.* **1989**, *111*, 3536.
(22) Lathrop, D.; Eckert, H. *Phys. Rev. B* **1991**, *43*, 7279.
(23) Lathrop, D.; Eckert, H. *J. Phys. Chem.* **1989**, *93*, 7895.
(24) Bjorholm, T.; Jakobsen, H. *J. Am. Chem. Soc.* **1991**, *113*, 27.
(25) Stebbins, J. F. *Science* **1989**, *245*, 257. Farnan, I.; Stebbins, J. F. *J. Am. Chem. Soc.* **1990**, *112*, 32.
(26) Blachnik, R.; Wickel, U. *Thermochim. Acta* **1984**, *81*, 185.
(27) Rollo, J. R.; Burns, G. R. *J. Non-Cryst. Solids* **1991**, *127*, 242.
(28) Keulen, E.; Vos, A. *Acta Crystallogr.* **1959**, *12*, 323.
(29) Lathrop, D.; Eckert, H. *J. Non-Cryst. Solids* **1988**, *106*, 417.

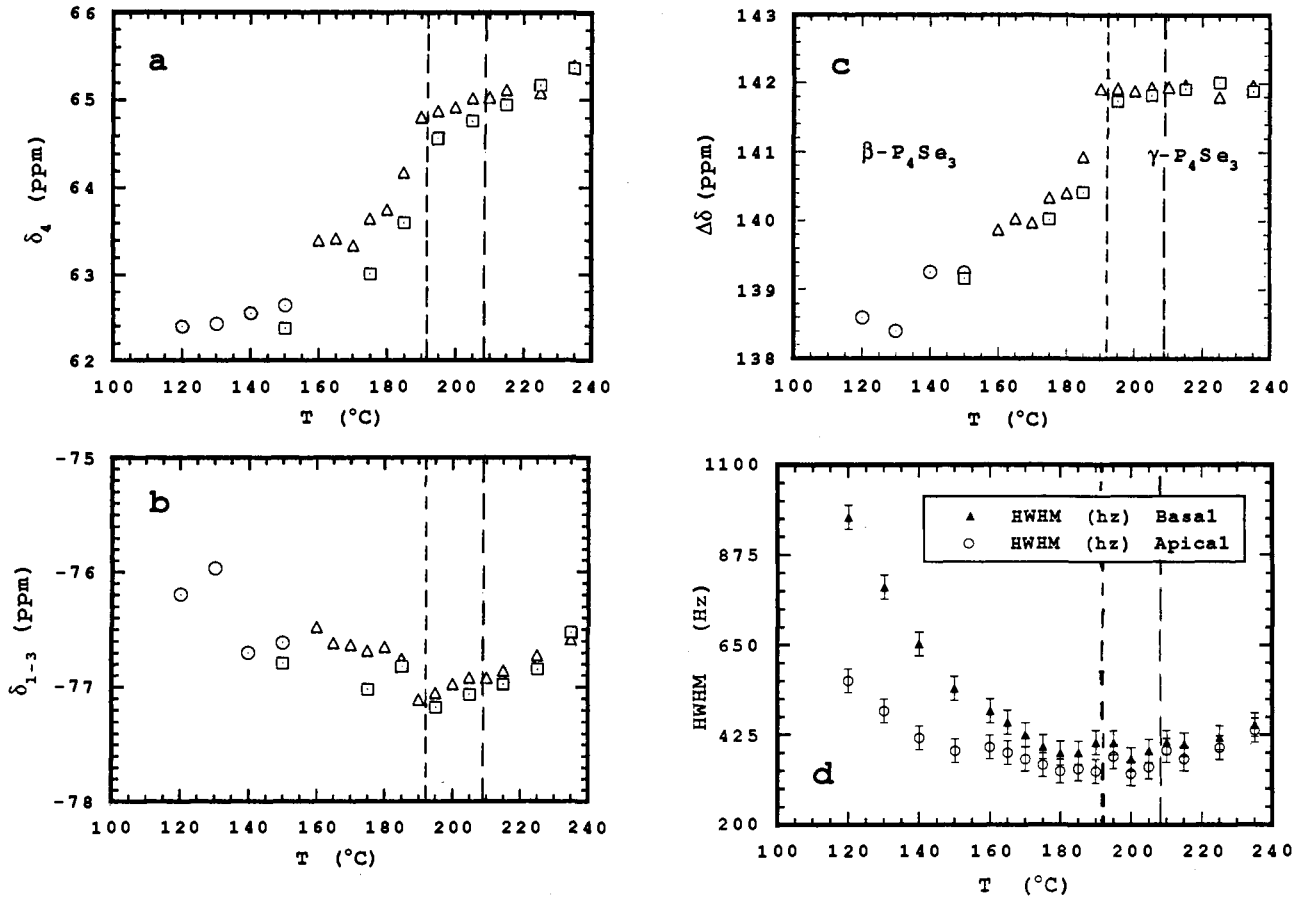

Figure 2. Temperature-dependent ^{31}P NMR studies of crystalline P_4Se_3 at 121.66 MHz: (a) chemical shifts for apical P atoms P_4; (b) chemical shifts for basal P atoms P_{1-3}; (c) chemical shift difference between the apical and the basal P atoms; (d) half widths at half maximum. Different symbols denote different samples studied at separate times. The dashed lines correspond to the β'–γ and the β–γ transition temperatures, 192 and 207 °C, respectively.

has been characterized by high-resolution ^{31}P NMR in the homologous compound P_4S_3.[30] The spectra of β- and β'-P_4Se_3 are essentially indistinguishable. However, the transition from the β or β' modifications to γ-P_4Se_3 manifests itself in a noticeable chemical shift effect (see Figure 2). The phase transition is detected most sensitively by the sharp change in the temperature coefficient $d(\Delta\delta)/dT$ of the chemical shift difference, $\Delta\delta = \delta_4 - \delta_{1-3}$. Compared to the chemical shift effect at the $\alpha \rightarrow \beta$ transition, the effect seen here is much smaller, because the phase transition is a rather subtle structural rearrangement only slightly modifying the strength of the intermolecular interactions between the rapidly reorienting molecules. (The exact structure of the γ-phase has yet to be determined by single-crystal X-ray diffraction.) Figure 2d reveals that a distinction between the β- and γ-phases is further possible on the basis of the line widths and their respective temperature dependences. We interpret the effect seen at the β- to γ-transition as indicative of a dramatic change in the molecular correlation time and/or the motional characteristics of the molecule.

Variable-Temperature ^{31}P NMR Studies of Phosphorus–Selenium Glasses. Figure 3 shows the ^{31}P NMR spectra of P–Se glasses containing 13, 30, 40, 45, and 48 atom % P over the whole temperature range studied. Room-temperature MAS ^{31}P NMR spectra of these glasses have been reported previously and are not shown here.[23] At and below the glass transition temperatures, the spectra are dominated still by broadening due to wide distributions and large anisotropies of chemical shifts and display resolution no better than previous wide-line or MAS NMR spectra. However, at temperatures well above T_g, the liquid eventually attains a viscosity consistent with motional narrowing and/or chemical shift averaging by rapid chemical exchange, resulting in partially resolved ^{31}P resonances which are assigned on the basis of comparison with spectra of model compounds and previous MAS NMR results obtained on these glasses.[23]

The spectra shown in Figure 3 are fundamentally different from those previously obtained for phosphorus–sulfur melts.[24] While in the P–S system, the spectra show the liquid to be a mixture of discrete P_4S_x molecules, NMR spectroscopy shows no evidence that analogous units play a significant role in phosphorus–selenium melts (or glasses). At lower temperatures, the spectra are dominated by a resonance around 135 ppm assigned to three-coordinated $PSe_{3/2}$ and $Se_{2/2}P$–$PSe_{2/2}$ units. The glass containing 13 atom % P shows a discernible shoulder on the upfield side, which is attributed to four-coordinated $Se{=}PSe_{3/2}$ groups previously identified by room-temperature MAS NMR studies.[23] As the temperature increases, this resonance disappears below 200 °C due to chemical exchange with the three-coordinated P atoms contributing to the main broad peak at 135 ppm. These results suggest that the $Se{=}PSe_{3/2}$ units are thermally very unstable, in agreement with recent studies on phosphorus–selenium films, where these units were shown to decompose under UV light illumination.[31]

Above 200 °C, the main broad resonance centered around 135 ppm splits into two peaks at 124 and 151 ppm. These two resonances cannot be assigned unequivocally to well-defined chemical species because, at these temperatures, the P atoms contributing to them are already involved in fast chemical exchange with the four-coordinated P atoms (and possibly other structures as well). As the temperature increases further, the distinct 124 and 151 ppm resonances are interchanging in a new

(30) Andrew, E. R.; Hinshaw, W. S.; Jasinski, A. *Chem. Phys. Lett.* **1974**, *24*, 399.

(31) Kumar, A.; Malhotra, L. K.; Chopra, K. L. *J. Non-Cryst. Solids* **1989**, *107*, 212.

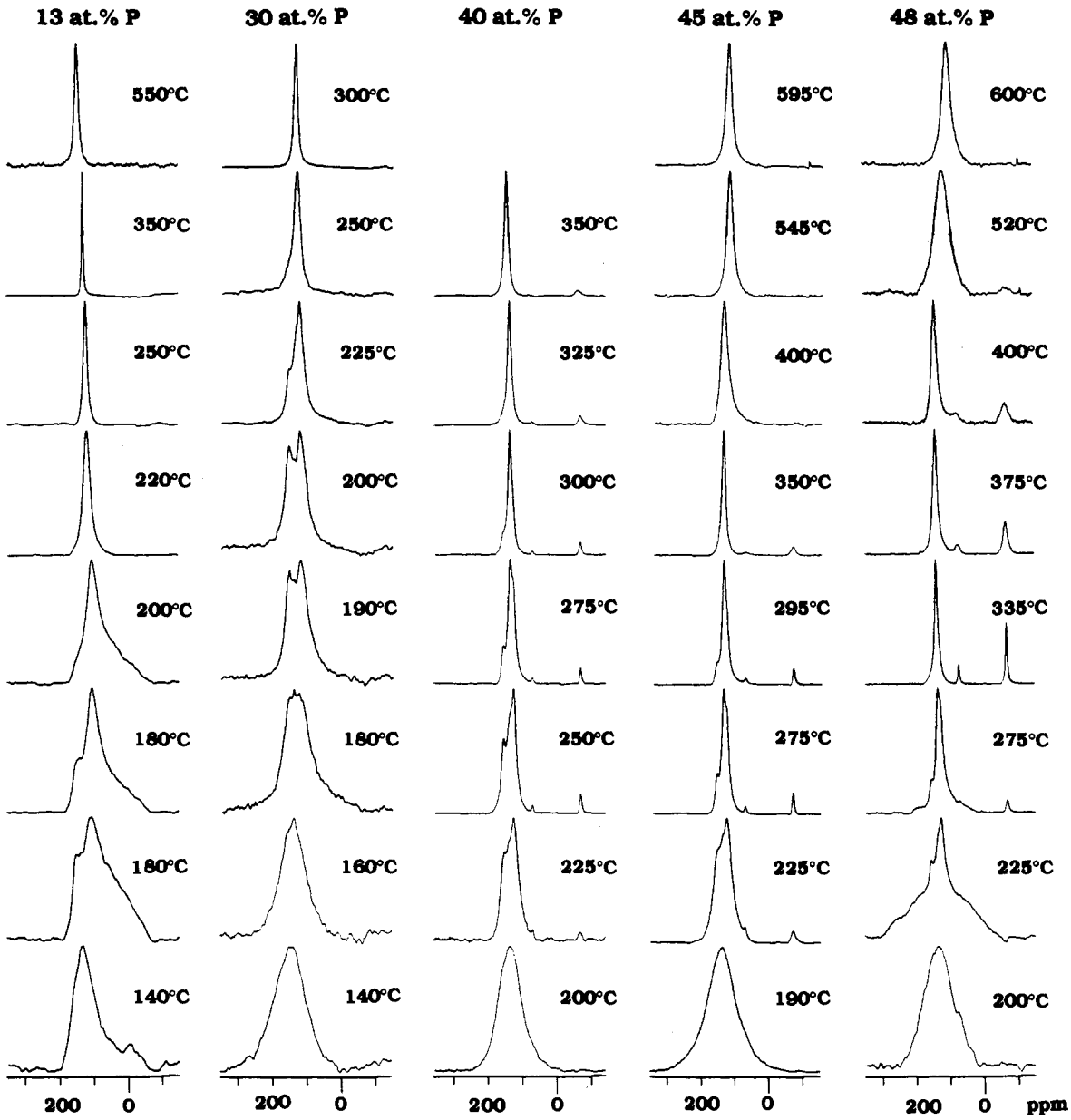

Figure 3. Variable-temperature ^{31}P NMR spectra of glasses and melts in the P–Se system. T_g's are 76, 86, 94, 140, 175 °C for glasses containing 13, 30, 40, 45, and 48 atom % P, respectively.

chemical exchange process, resulting in the gradual appearance of a single Lorentzian line around 140 ppm.

Above 200 °C, melts with P contents ≥ 40 atom % clearly display the resonances near 70 and −70 ppm belonging to molecular P_4Se_3 units, while no such units are seen at lower phosphorus contents. As can be seen in Figure 3, there is evidence that the fraction of P atoms contributing to the P_4Se_3 resonance increases as the temperature increases. This is particularly obvious in the spectrum of the 48 atom % P glass, where the P_4Se_3 spectrum grows rapidly at the expense of a broad pattern at the base of the ^{31}P resonance. These temperature-dependent changes are attributed to a thermally activated depolymerization process resulting in the formation of P_4Se_3 molecules in the melt. Figure 4 illustrates an example for this envisioned process. Room-temperature MAS NMR spectra confirm the complete absence of P_4Se_3 molecules in all of the glasses studied, except those with P contents ≥ 50 atom % P.[21-23] Figure 5 summarizes the fraction of P atoms contributing to molecular P_4Se_3 as a function of temperature for glasses containing 40, 45, and 48 atom % P. As expected, the fraction of P atoms ultimately present in the form of P_4Se_3 at high temperatures increases with increasing phosphorus concentration.

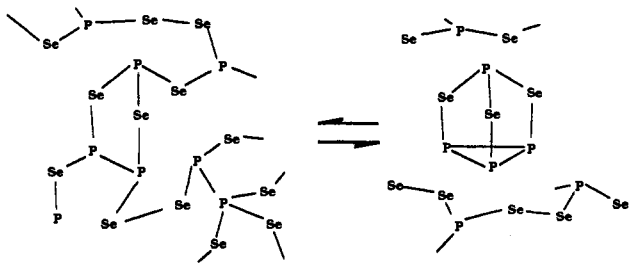

Figure 4. Schematic of a melt depolymerization process resulting in the formation of molecular P_4Se_3.

Note that within the temperature range 200 °C ≤ T ≤ 400 °C the ^{31}P NMR spectra reveal that the molecular P_4Se_3 species are isolated and distinct, indicating that, in this motional regime, chemical exchange processes involving P_4Se_3 with other types of phosphorus-containing units are slow on the NMR time scale. Above 400 °C, however, there is clear evidence for line-shape averaging by fast chemical exchange, affecting position, width, and temperature dependence of the dominant ^{31}P resonance. This line-shape averaging is particularly well documented in Figure

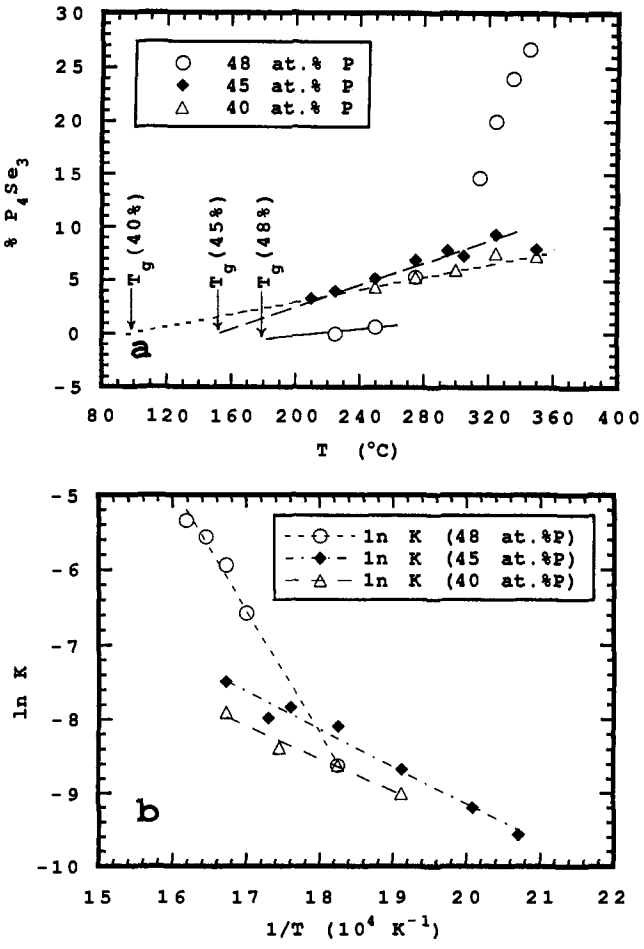

Figure 5. (a) Temperature and composition dependence of the P_4Se_3 concentration in phosphorus–selenium melts. (b) Arrhenius plot of the equilibrium constant K as defined in the text. T_g's are 94, 140, and 175 °C for glasses containing 40, 45, and 48 atom % P, respectively.

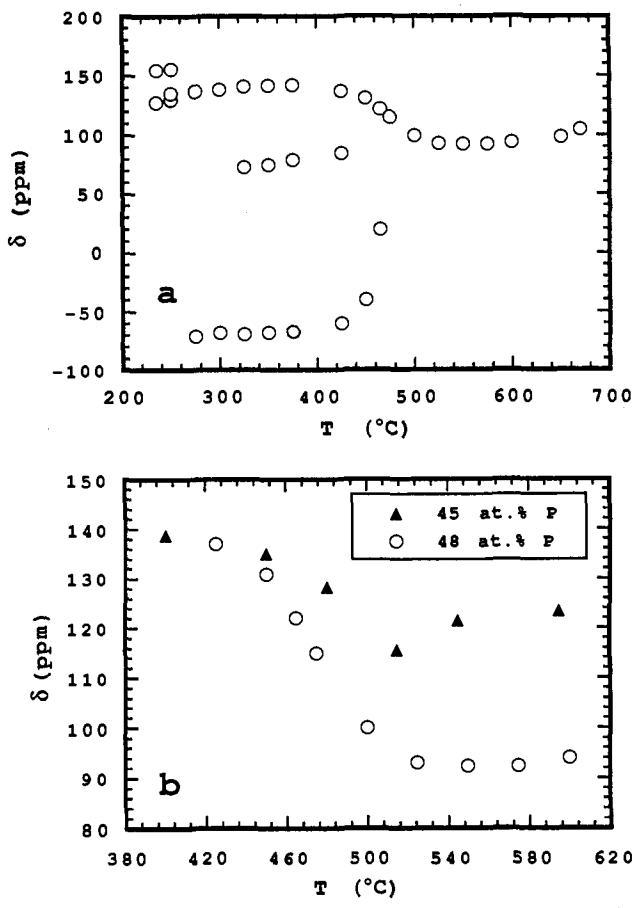

Figure 6. (a) Temperature-dependent evolution of the ^{31}P chemical shifts of the ^{31}P resonances belonging to P_4Se_3 and the molten glass matrix. (b) Temperature dependence of the ^{31}P chemical shifts associated with the molten glass matrix at high temperatures for glasses containing 45 and 48 atom % P, respectively.

6a, which depicts the temperature dependence of the chemical shifts of the various species present. The effect of the P/Se ratio in the glass on the P_4Se_3 fraction can be seen in Figure 6b. As expected, the chemical shift resulting in the fast-exchange limit is significantly further upfield in the glass containing 48 atom % P compared to the one containing 45 atom % P.

Discussion

The variable-temperature-NMR results shown in Figures 3, 5, and 6 show that the structure of P–Se melts is affected by two distinct temperature-dependent processes: (a) destruction of tetrahedral Se=$PSe_{3/2}$ groups below 200 °C and (b) the creation of P_4Se_3 molecules due to network depolymerization at temperatures above 200 °C. In addition, the spectra are affected by thermally activated chemical exchange phenomena in the 200–300 °C range due to a process currently not well understood, but unrelated to the presence of molecular P_4Se_3. Finally, at temperatures above 400 °C, the chemical exchange between P_4Se_3 molecules and the P atoms of the molten matrix is sufficiently rapid to affect the ^{31}P NMR spectra. In the discussion to follow, we will (1) examine the equilibria resulting in the creation of P_4Se_3 molecules in more quantitative detail and (2) extract kinetic information about the high-temperature chemical exchange process with the help of line-shape simulations.

Temperature-Dependent Creation of Molecular P_4Se_3 Units in P–Se Glasses. Figure 5a depicts numerically the concentration of P_4Se_3 as a function of temperature for melts containing 40, 45, and 48 atom % P. In agreement with previous MAS NMR results, there are no molecular P_4Se_3 units discernible in the NMR spectra of glasses containing less than 50 atom % P at temperatures below 200 °C. However, P_4Se_3 begins to form near 250 °C, and its concentration increases linearly in all of the glasses. In the case of the 48 atom % P sample, molecular P_4Se_3 appears to be formed by two distinct mechanisms: the process operative in the glasses with lower P contents, as well as a process involving the decomposition of a second glass component, presumably solid amorphous P_4Se_4, which gives rise to a broad resonance seen in Figure 3 at T = 225 and 275 °C but appears to be absent in glasses with lower P concentrations. Due to the presence of this component, at lower temperatures the formation of P_4Se_3 initially appears to be retarded but then commences with a temperature-dependent slope far greater than that seen in either the 40 or 45 atom % P glasses. To analyze the temperature-dependent evolution of the NMR spectra seen in Figure 3, we postulate that the process illustrated in Figure 4 can be defined by the melt equilibrium

$$P_xSe_{1-x} \Leftrightarrow aP_4Se_3 + aP_{((x/a)-4)}Se_{(((1-x)/a)-3}$$

The equilibrium constant for this process is easily calculable as

$$K = a^2/(1-a)$$

where a is the concentration of P_4Se_3 units in the melt, as determined by experiment at each temperature. Arrhenius plots showing K as a function of inverse temperature are shown in Figure 5b for the 40, 45, and 48 atom % P glasses. At temperatures above T_g, but below $2T_g$, the equilibrium of P_4Se_3 with the polymeric melt is characterized by a equilibrium constant that is weakly temperature dependent for the glasses containing 40 and 45 atom % P, with enthalpies of reaction of 37 and 42 ± 5

kJ/mol, respectively. For the glass containing 48 atom % P, however, we observe a strong bimodal temperature dependence of K. At temperatures below the decomposition temperature of the P_4Se_4 glass component (~275 °C), K is weakly temperature dependent, corresponding to an enthalpy of reaction of 40 ± 20 kJ/mol (the rather large error here is due to the inherent difficulty of integrating peaks whose signal to noise ratios are close to unity). By contrast, the analogous description of the P_4Se_4 decomposition as an equilibrium process results in a strongly temperature-dependent equilibrium constant, corresponding to a reaction enthalpy of 136 ± 7 kJ/mol.

Chemical Exchange between Molecular P_4Se_3 and the Molten-Glass Matrix. The theory of chemical exchange effects on liquid-state-NMR spectra is well established and can be applied here to study the kinetics of the high-temperature interconversion process observed at $T \geq 400$ °C. Simulation of the ^{31}P NMR spectra is based on methods described in detail elsewhere[32] using modified Bloch equations for a system of three spin-$^1/_2$ resonances:

$$\frac{dM_1}{dt} = -\alpha_1 M_1 - iC_1 + k_{31}M_3 + k_{21}M_2 - M_1(k_{13} + k_{12})$$

$$\frac{dM_2}{dt} = -\alpha_2 M_2 - iC_2 + k_{32}M_3 + k_{12}M_1 - M_2(k_{21} + k_{23})$$

$$\frac{dM_3}{dt} = -\alpha_3 M_3 - iC_3 + k_{23}M_2 + k_{13}M_1 - M_3(k_{31} + k_{32})$$

where $\alpha_m = T_{2m}^{-1} - i(\omega_m - \omega)$, C_m is the fractional population of each spin species as defined in ref 32, and k_{mn} is the rate constant for exchange between sites m and n, with $1 \leq m$ or $n \leq 3$. The three spin species are identified with (1) the P atoms contributing to the liquid matrix ($\delta \sim 140$ ppm), (2) the apical P atoms of molecular P_4Se_3 ($\delta \sim 74$ ppm), and (3) the basal P atoms of molecular P_4Se_3 ($\delta \sim -67$ ppm). Solving the three coupled differential equations at steady-state conditions for this particular case yields the following expression for the line shape $l(\omega)$:

$$l(\omega) = \mathrm{Im}\{M_{\mathrm{total}}(\omega)\} = \mathrm{Im}(G/|\Delta|)$$

where

$$G = G_1 + G_2 + G_3$$

and

$$G_1 = \begin{bmatrix} iC_1 & (C_1/C_3)k & (C_1/C_3)k \\ iC_2 & -(\alpha_2 + (C_1/C_3)k) & 0 \\ iC_3 & 0 & -(\alpha_3 + (C_1/C_3)k) \end{bmatrix}$$

$$G_2 = \begin{bmatrix} -(\alpha_1 + (^4/_3)k) & iC_1 & (C_1/C_3)k \\ (^1/_3)k & iC_2 & 0 \\ k & iC_3 & -(\alpha_3 + (C_1/C_3)k) \end{bmatrix}$$

$$G_3 = \begin{bmatrix} -(\alpha_1 + (^4/_3)k) & (C_1/C_3)k & iC_1 \\ (^1/_3)k & -(\alpha_2 + (C_1/C_3)k) & iC_2 \\ k & 0 & iC_3 \end{bmatrix}$$

$$\Delta = \begin{bmatrix} -(\alpha_1 + (^4/_3)k) & (C_1/C_3)k & (C_1/C_3)k \\ (^1/_3)k & -(\alpha_2 + (C_1/C_3)k) & 0 \\ k & 0 & -(\alpha_3 + (C_1/C_3)k) \end{bmatrix}$$

(32) Sandstrom, J. *Dynamic NMR Spectroscopy*; Academic Press: New York, 1982. Kaplan, J.; Fraenkel, G. *NMR of Chemically Exchanging Systems*; Academic Press: New York, 1980.

Table I. Simulation Parameters and Resulting Exchange Rate Constants[a]

T (°C)	δ_m (ppm)	δ_b (ppm)	δ_a (ppm)	$1/T_{2,m}$ (kHz)	$1/T_{2,b\,a}$ (kHz)	% P_4Se_3	k (s^{-1})
365	143	–67	74	3.46	1.22	25.3	763
385	144	–66	75	3.10	1.53	25.5	1170
400	144	–66	75	3.05	1.53	25.5	1980
415	145	–66	75	3.21	2.04	27.7	3130
425	146	–65	76	3.41	2.29	25.5	4170
450	147	–65	76	4.07	3.05	25.5	8140
475	149	–64	76	5.09	4.07	25.5	15300
525	150	–64	76	5.60	7.12	31.1	55960
550	151	–64	77	6.10	9.67	31.1	101800

[a] δ_m and $1/T_{2,m}$ refer to the glass resonance representing three-coordinate P units derived from extrapolation of temperature dependence before the onset of exchange and comparison to low P content glasses without P_4Se_3. δ_b, δ_a, and $1/T_{2,b\,a}$ refer to the basal and apical phosphorus in dissolved P_4Se_3 obtained from VT studies of P_4Se_3.

with

$$k = k_{13},\ k_{12} = {}^1/_3k_{13} = {}^1/_3k,\ k_{m1} = (C_1/C_m)k_{1m}$$

and

$$k_{23} = k_{32} = 0$$

Input values of the above parameters are listed in Table I. In the slow-exchange limit, Lorentzian line shapes are assumed for all signal components. For the signals arising from P_4Se_3, this assumption is justified because the rapid molecular reorientation of this near-spherical molecule leads to complete averaging of the chemical shift anisotropy. For the signal attributed to the "polymeric" phosphorus species, Lorentzian line shapes are justified as well, because the chemical shift anisotropy is already averaged by the other chemical exchange processes occurring at lower temperatures (see above). At the (higher) temperatures where exchange with the P_4Se_3 molecules affects the NMR spectra, the situation is thus slightly different to that for ^{29}Si in polymeric silicate liquids, where averaging of the chemical shift anisotropy is part of the same process that leads to exchange among structural species.[25] Temperature dependences of the P_4Se_3 chemical shifts and T_2's were estimated by comparison to the temperature-dependent studies of P_4Se_3 and, for the P atoms in the molten matrix, by extrapolating their temperature dependences within the temperature region below the onset of chemical exchange with P_4Se_3. The fractional contribution of molecular P_4Se_3 is slightly higher than that obtained by integration at lower temperatures and is quantitatively consistent with the temperature-dependent equilibrium constant of P_4Se_3 creation discussed in the previous section. The only variable, then, is k, the rate constant for the exchange between the P atoms in the P_4Se_3 molecule and those in the molten matrix. The model employed here neglects mutual exchange between the two kinds of P atoms in the P_4Se_3 molecule. This assumption is justified in view of high-temperature studies of molten P_4Se_3 showing the absence of chemical exchange effects up to 600 °C. Since the spectral resolution obtained is not sufficient to resolve homonuclear scalar coupling between the P resonances in P_4Se_3, this interaction is not included in the simulations.

Figure 7 shows the ^{31}P NMR spectra at 81.0 MHz of 48 atom % P P–Se glass above 350 °C along with their simulations, revealing generally excellent agreement. An Arrhenius plot of the rate constant is shown in Figure 8, from which we determine the activation energy for this exchange process to be 116 ± 6 kJ/mol. By extrapolation, we find that near T_g the rate of chemical exchange is on the order of a few minutes. While such low rates leave the NMR line shapes unaffected, the exchange process is certainly sufficiently fast on the time scale of the temperature-dependent NMR measurements (30–60 min) to allow full equilibration between the P_4Se_3 molecules and the other

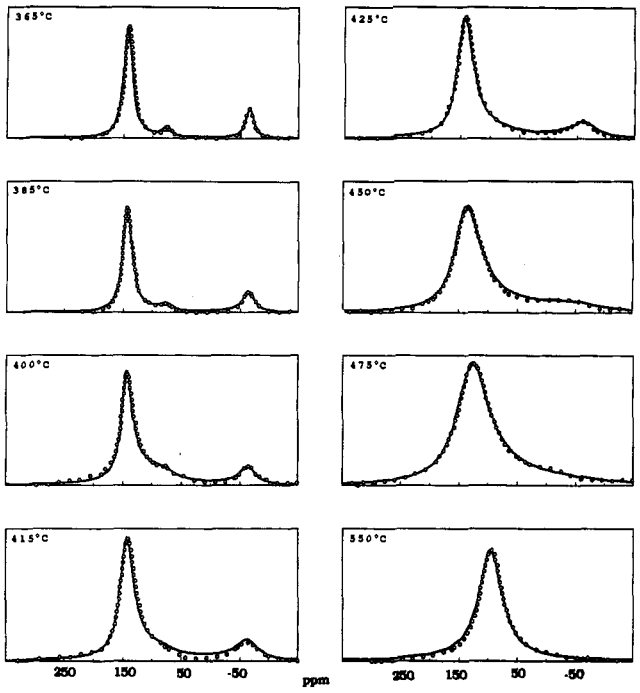

Figure 7. Comparison between experimental (circles) and simulated (solid lines) ^{31}P NMR spectra assuming chemical exchange on the NMR time scale for the apical and basal P atoms with the molten matrix.

P-containing structures in the glass at each temperature. Thus, we can conclude that the glass depolymerization process monitored by NMR above T_g reflects an equilibrium situation at each temperature.

Conclusions

The results of the present study illustrate the power of high-temperature in situ ^{31}P NMR for providing intimate details about the thermodynamic and kinetic processes occurring in phosphorus–selenium melts above the glass transition. Using this approach, it has been possible to quantify the extent to which P_4Se_3 molecules are formed in the molten state at elevated temperatures due to temperature-dependent depolymerization equilibria, and to characterize the kinetics of interchange between molecular P_4Se_3 and the molten-glass matrix. Extrapolation of the kinetic data to

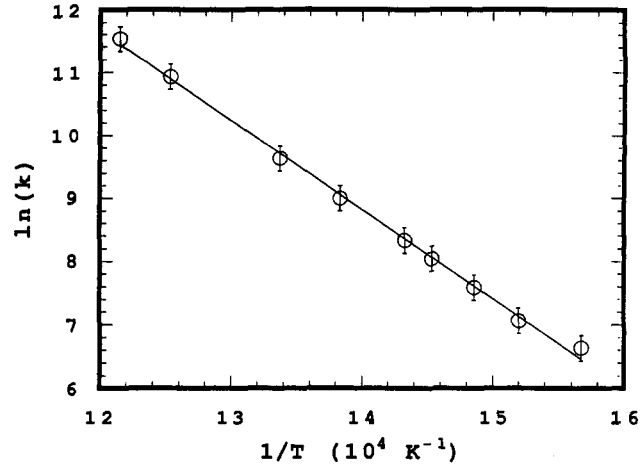

Figure 8. Arrhenius plot of the chemical exchange rate constants extracted from the best-fit simulations of the variable-temperature NMR line shapes.

temperatures near the glass transition temperatures suggests that T_g in these chalcogenide glasses is associated with bond breakage/bond formation processes in a fashion similar to those found in silicate glasses.

In addition, extrapolation of the temperature-dependent P_4Se_3 species concentrations to T_g illustrates that their concentrations in the glassy states are minimal except at compositions near the edge of the glass-forming region (≥50 atom % P). Nevertheless, the fact that P_4Se_3 molecules are allowed to form suggests the presence of corresponding polymerized precursor states in the glass structure (see Figure 4), at P contents of 40 atom % and above. The NMR quantification of molecular P_4Se_3 at high temperatures suggests that the concentrations of such precursor states are rather low, except in the immediate vicinity of the glass-forming border. Thus, the present high-temperature data confirm that intermediate-range order and clustering only play a minor role in the structural organization of selenium-rich phosphorus–selenium glasses. As a result, and in direct contrast to selenium-deficient glasses, selenium-rich glasses should not be viewed as zero-dimensional.

Acknowledgment. This research was supported by NSF Grant DMR-8913738 and by a grant from the UCSB Academic Senate. The authors thank Mr. Tom Tepe and Dr. Regina Francisco for assistance with the sample preparation.